

Episodic Strain Accumulation in Southern California

Stresses have increased across thrust faults
in the central Transverse Ranges.

Wayne Thatcher

A remarkable episode of aseismic crustal uplift occurring between 1960 and 1974, covering at least 12,000 square kilometers of southern California, and totaling 0.15 to 0.25 meter, has recently been uncovered by the synthesis of a large number of repeated precise level line measurements (1). Sharply contrasted with this epoch is the slow regular rate of crustal deformation observed in many tectonically active parts of California, deformation that is tacitly assumed to be the primary mode of earthquake strain accumulation. Measured against this experience, the magnitude, rapidity, and areal extent of the recent uplift are surprising to most earth scientists, raising compelling questions concerning its origin, mechanism, and possible relation to impending earthquakes.

It is unlikely that such an unusual uplift event would occur without some correspondingly anomalous horizontal deformation accompanying it. Therefore, I have reexamined data from horizontal control surveys carried out in the western half of the uplifted region during 1932 to 1975, and present here a summary of the principal results of this work. Viewed jointly, the horizontal and vertical geodetic data suggest some general implications of the uplift, draw attention to its possible relation to thrust-type earthquakes like the 1952 Kern County and 1971 San Fernando events (Fig. 1), and suggest a plausible interpretation for some previously reported local uplift that occurred prior to the 1971 earthquake.

Horizontal Data Analysis

The spatial coverage and survey dates of the observations used here are shown in Fig. 1, along with the 0.15-m uplift contour. The data (2-4) consist largely of

triangulation surveys, repeated measurements of the angular separation of permanent survey monuments. The changes in these angles between surveys depend on the shear strain changes that have occurred, and thus the angle changes may be used to deduce the orientation and average rate of shear straining during the time interval between surveys (5, 6). This is done here by the method of least squares (7). The only assumption made in this analysis is that the strain field is spatially uniform over the region within which angle changes are used to determine it. Thus, standard deviations from the least squares fit represent both data errors and any real departures from the assumed uniformity of the strain field. A second implicit assumption is that the rate and orientation of the field have remained constant throughout the intersurvey time interval. For the data examined here, this assumption is probably invalid in at least one instance, and this departure introduces a subtle complication into the interpretation of these particular observations.

Normal and Anomalous Shear Straining

When sufficient constraints exist, it can be shown that most of the anomalous shear straining that can be directly related to the uplift occurred between 1959 and 1963. This is best demonstrated by considering measurements made from 1932 to 1967 within about 30 km of the San Andreas fault. This subregion has been chosen both because of the density and relative frequency of measurements and because here, close to the San Andreas fault, it is easiest to distinguish unambiguously between normal and anomalous shear straining. Right-lateral shear strain rates and orientations for two lumped intervals, 1941 to 1959 and

1932 to 1952 (normal), and 1959 to 1967 and 1952 to 1963 (anomalous), are plotted in Fig. 2 and listed in Table 1.

Consider first the normal shear strains: orientations are all within 2 standard deviations of the local strike of the San Andreas fault, 105° to 115° in this region, and rates are all close to 0.3×10^{-6} year $^{-1}$, values typical of secular strain accumulation along several other portions of the San Andreas system (3, 8, 9). The pattern of shear straining that occurred during the normal time interval is just that predicted by simple models of strain accumulation on the San Andreas fault in this region: deformation results from slow, steady aseismic slippage of 30 to 40 millimeters per year on the San Andreas fault system north and south of the partially or completely locked bend of the fault between 35° and 34° N (Fig. 1) (3, 10).

Shear straining from 1959 to 1967 and 1952 to 1963 shows significant departures from that determined for the earlier time intervals. Comparing results for 1941 to 1959 with those for 1959 to 1967 (Fig. 2 and Table 1) reveals significant differences in the orientation of right-lateral shear straining in subregions B and C. Other data for the 1959/67 net (Fig. 1) from areas adjacent to subregions B and C show features which corroborate the anomalous 1959/67 shear straining given in Table 1. These two sets of data provide the most definitive evidence for unusual shear straining during the development of the uplift. Measurements from the north-south 1932/52/63 net (Fig. 2 and Table 1) provide additional constraints on the anomalous horizontal deformation, but for these data the effects of the anomalous strain field are more subtle. Indeed, at first glance they appear to contradict the 1959/67 results from the 1941/59/67 net: with the possible exception of subregion D (Table 1), none of the shear strain rates during the period 1952 to 1963 is significantly greater than zero, and the orientation, with much scatter, varies 30° to 50° from the trend of the San Andreas fault. This departure from the presumed normal deformation of 1932 to 1952 has two possible explanations: (i) that shear straining had in fact essentially ceased during the interval 1952 to 1963, or (ii) that during this interval a second anomalous strain field was destructively interfering with the normal secular field.

The first alternative, although not unambiguously excluded, does not account for the change in shear strains

The author is a geophysicist at the National Center for Earthquake Research, U.S. Geological Survey, Menlo Park, California 94025.

Table 1. Rate ($\dot{\epsilon}$, $\mu\text{strain/year}$) and orientation (ψ , degrees) of right-lateral shear strain for normal (1941 to 1959 and 1932 to 1952) and anomalous (1959 to 1967 and 1952 to 1963) time intervals. Values are means \pm 1 standard deviation calculated from least squares fits of the data. Values in parentheses have large standard deviations and by themselves are not considered statistically significant. Residuals are observed minus secular values; the secular field assumed is $\dot{\epsilon} = 0.3 \mu\text{strain/year}$ parallel to the local strike of the San Andreas fault. Rates and orientations are plotted in Fig. 2.

Sub-region	Normal time intervals		Anomalous time intervals		Residuals	
	$\dot{\epsilon}$	ψ	$\dot{\epsilon}$	ψ	e	ψ
			<i>1941/59/67 net</i>			
A	0.10 ± 0.11	(146 ± 40)	0.39 ± 0.14	106 ± 14	(0.7 ± 1.1)	(105 ± 35)
B	0.34 ± 0.20	87 ± 18	0.36 ± 0.10	11 ± 10	4.7 ± 0.8	14 ± 6
C	0.32 ± 0.13	93 ± 12	0.69 ± 0.19	136 ± 8	4.8 ± 1.5	148 ± 12
			<i>1932/52/63 net</i>			
D	0.27 ± 0.08	104 ± 11	(0.26 ± 0.16)	(168 ± 28)	4.1 ± 1.7	1 ± 13
E	0.30 ± 0.09	118 ± 13	(0.11 ± 0.17)	(170 ± 56)	3.2 ± 2.0	6 ± 20
F	0.28 ± 0.08	109 ± 12	(0.06 ± 0.12)	(48 ± 70)	2.8 ± 1.3	20 ± 18
G	0.30 ± 0.09	111 ± 12	(0.11 ± 0.13)	(148 ± 50)	2.5 ± 1.5	1 ± 16
H	0.19 ± 0.06	92 ± 9	(0.11 ± 0.12)	(140 ± 30)	2.2 ± 1.3	179 ± 18

between the intervals 1941 to 1959 and 1959 to 1967 (Table 1). Therefore, I have assumed that the normal and anomalous fields are superposed from 1952 to 1963. With this assumption, the anomalous field may be obtained by simply subtracting the expected shear strains from the actual observed field (note, however, that this involves the subtraction of two tensor fields). This residual shear straining is shown in Table 1 for both triangulation nets. The total shear straining from 1959 to 1967 and 1952 to 1963 is roughly comparable, averaging about 4 microstrains, which suggests that most (although probably not all) of the anomalous straining occurred during the common 3½-year interval from late 1959 to mid-1963. Even assuming that this deformation was uniform in time from 1959 to 1963, its rate is a factor of 4 greater than the rate of normal secular shear straining. Furthermore, comparison with the independent leveling data (1), which indicate that most of the episodic uplift in this region occurred in 1961 to 1962,

suggests that horizontal deformation rates may have been significantly greater during this short time interval.

Precise laser-ranging distance measurements carried out from 1971 to 1975 (see Fig. 1) demonstrate (3) that shear straining had returned essentially to normal by this time interval, if not earlier. Other Geodimeter measurements sparsely scattered throughout the area of Fig. 1 have been repeated at 1- to 7-year intervals from 1959 to 1968 (11) and potentially offer further constraints on the anomalous horizontal deformation. Unfortunately, these data are contaminated by rather large systematic errors (12), which severely limit their value (13).

Implications

The character of the anomalous shear straining and its relation to the uplift are conveniently demonstrated by plotting the orientation of the maximum compressive strain axis (14) on the same map as

the uplift contours (Fig. 3). Axes plotted include those determined from the data for 1952 to 1963 and 1959 to 1967, corrected wherever possible for the secular shear straining (shown with dots in Fig. 3), along with uncorrected results for 1953 to 1963 (after the Kern County earthquake) from the east-west arc labeled 1932/52/53/63 in Fig. 1 (4). Even conceding several significant departures, the compressive strain axes show a clear tendency to orient themselves perpendicular to the uplift contours. This characteristic pattern is preserved even where the contours locally trend east-southeast near the center of Fig. 3. Thus the uplift, whatever its detailed mechanism, is closely related to the north-south to northeast-southwest horizontal compression.

Several characteristics of the anomalous horizontal deformation divert attention away from the San Andreas system and focus it on the north-dipping thrust faults of the Transverse Ranges (within the map area of Fig. 1, these faults lie near the southern boundary of the uplifted region). The orientation of compressive strains nearly normal to the San Andreas suggests that the uplift has produced little, if any, shear strain accumulation across this fault, and may indeed have locked it locally, impeding slippage (14). In contrast, this same strain field increased shear strains across the north-dipping boundary faults of the Transverse Ranges. On this basis I view the uplift, whatever its detailed mechanism, as a nearly impulsive episode of strain accumulation on these range-front thrust faults.

If this interpretation is correct, the uplift has increased the likelihood of potentially destructive earthquakes on these faults, although the geodetic data examined here cannot be used to estimate when these events might occur.

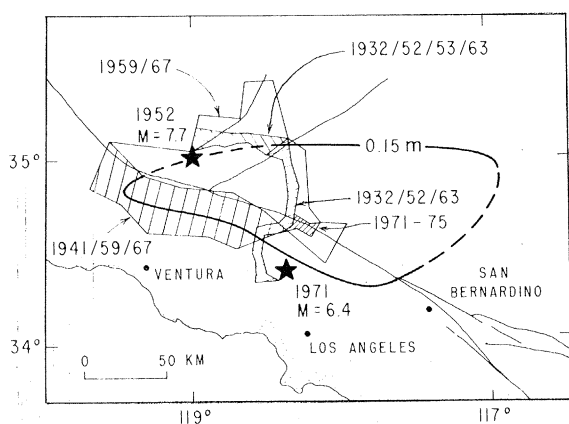
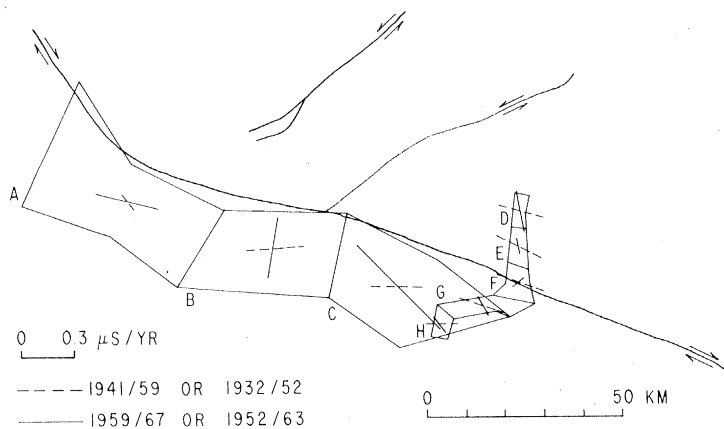


Fig. 1 (left). Location and survey dates of horizontal control data used in this study. Epicenters of the 1952 Kern County and 1971 San Fernando earthquakes are shown by stars; M = magnitude. The 0.15-m uplift contour is shown for reference. Fig. 2 (right). Comparison of right-lateral shear strain rates for two lumped time intervals, 1941 to 1959 and 1932 to 1952 (solid lines), and 1959 to 1967 and 1952 to 1963 (dashed lines). All plotted rates are listed in Table 1.



However, estimates of the shear strain increment required to produce rupture in crustal fault zones provide a useful yardstick against which to measure the importance of this latest episode of deformation. Geodetic surveys carried out in the source regions of major earthquakes in Japan and California suggest (15) that shear strains across active crustal faults must exceed 50 μ strain before rupture will occur. Within the uplift region, horizontal control coverage is somewhat to the north of the active range bounding thrust faults; still, the inferred uplift-related shear strains amount to only 2 to 5 μ strain. Thus, even allowing for some decrease in straining away from the faults, this latest uplift epoch incremented shear strains significantly less than the amount required for catastrophic failure. An obvious corollary of this interpretation is that uplifts even as large as the recent one need not be correlated one-to-one with major earthquakes. Thus, for example, a possibly similar epoch of rapid uplift that occurred between 1897 and 1914 (1) was not followed by any significant earthquakes.

Suggestive evidence does, however, point to a relation between the recent uplift and two thrust earthquakes located adjacent to the uplifted region (Fig. 1). The 1952 Kern County earthquake was associated with more than 50 km of surface ground breakage and left-lateral-thrust motion across the White Wolf fault, which dips moderately to the south-southeast in this region. The compressive strain axes determined from 1953–1963 triangulation data in this region (Fig. 3) almost certainly represent a postseismic adjustment to the 1952 shock (4). However, again, as near the center of the uplift region, the compressive axes tend to be orthogonal to the broad-scale trend of the uplift contours. Arguably, this relation could be fortuitous. However, the leveling data show (1) that the uplift began developing at its western boundary, immediately adjacent to the southwestern edge of the Kern County aftershock zone. Therefore, while not conclusive, the available evidence supports the conjecture that the 1952 earthquake and its aseismic after-effects may be causally related to the initiation of the uplift.

As for the 1971 San Fernando earthquake, a good case can be made that it locally relieved uplift-related shear strains. This earthquake was accompanied by 15 km of surface rupturing on the San Fernando fault, an east-west striking, north-dipping thrust typical of the active faults that form the southern boundary of the Transverse Ranges. The compressive stress axis for this earth-

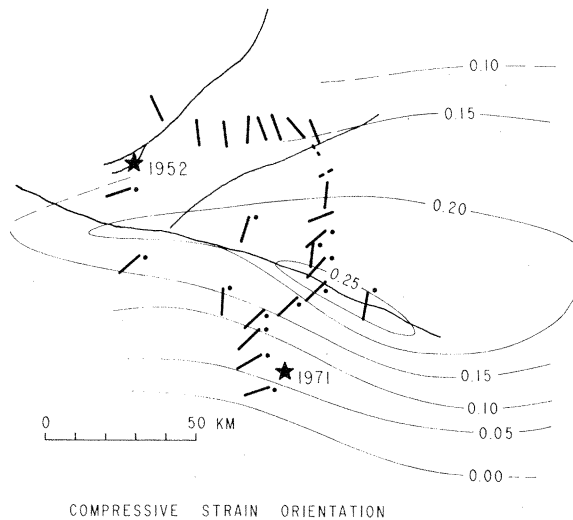


Fig. 3. Orientation of the compressive strain axes determined from triangulation data for 1952 to 1963 and 1959 to 1967. Superimposed are the independently derived uplift contours given by Castle *et al.* (1). Lines shown with dots have been corrected by subtracting out the normal secular shear strains (see text). Dashed lines indicate less reliably determined orientations. Stars give epicenters of 1952 ($M = 7.7$) and 1971 ($M = 6.4$) earthquakes.

quake, determined from its fault plane solution (16), is almost horizontal and trends northeast-southwest, virtually parallel to the local compressive strain orientations inferred from the 1952–1963 triangulation data (Fig. 3). Of course, the restricted areal extent of the 1971 rupture implies that accumulated shear strains were relieved over only a small fraction of the entire uplift region.

Although earthquake risk in the uplift region depends significantly on the level of strain accumulation reached before the uplift began, which is unknown, a relative estimate of this level might be obtained from in situ measurements of the orientation of the absolute stress field (17). Principal stress axes oriented parallel to the anomalous (1959–1963) principal strain axes would suggest that range-front thrust faults currently have a higher earthquake potential than do the right-lateral strike-slip faults of the San Andreas system. Of course, imminence of either type of earthquake depends on both the absolute stress level and the shear strength of the faults involved, neither one of which is either known at present or straightforward to determine experimentally.

Despite the fact that several significant implications of the uplift follow directly from consideration of the horizontal and vertical geodetic observations themselves, a precise mechanical model of the uplift remains clearly desirable. In constraining possible kinematic models, much depends on whether the lithosphere in southern California is 50 to 100 km thick, as is usually assumed, or only 30 to 40 km thick, as suggested by recent seismic evidence (18). Assuming a thick lithosphere, aseismic slip below about 30 km on a megathrust dipping north beneath the Transverse Ranges can account for the gross features of the geodetic data. On the other hand, if the litho-

sphere is decoupled from the asthenosphere at shallow depths, compression of a thin plate may be a more appropriate mechanism (19).

Localized Preseismic Uplift

Regardless of the exact mechanism responsible for the uplift, more localized episodic tilting that occurred between 1965 and 1971 near the epicenter of the 1971 San Fernando earthquake (20) appears to be ascribable to aseismic slip propagation toward the eventual seismic rupture zone. A 40-km-long level line (labeled CB in Fig. 4a) centered 40 km northwest of the 1971 epicenter was surveyed in 1964, 1965, 1968, 1969, and 1971 (after the earthquake) and showed an unusual sequence of tilt reversals between 1965 and 1971. In 1964 and 1965, a broad upwarping extended along the entire leveling route ABC (Fig. 4a) and reached a maximum amplitude of about 60 mm at a point centered roughly halfway between B and C. Along line CB, this was followed by a sharp tilt down to the south from 1965 to 1968, an even sharper tilt down to the north in 1968 and 1969, and finally a tilt to the south once again from 1969 to 1971 (Fig. 5). Tilts averaged nearly 3 microradians over a 25-km-long section of the line, almost an order of magnitude larger than the estimated uncertainty of these first-order measurements (6, 21). The pattern of tilting that occurred from 1965 to 1971 is precisely that expected from up-dip aseismic slip propagation on a north-dipping thrust fault, as shown schematically in Fig. 4b. The up-dip slip propagation produces an uplift profile similar to that of a wave breaking to the south toward the eventual 1971 surface rupture. The line CB views only a portion of this wave during each time interval, but

the sequence of tilts shown by this simple model matches the observed pattern quite well.

The detailed fit of model to data for one particular slip distribution is shown in Fig. 5. The model assumed is an east-west striking, 30° north-dipping, two-dimensional thrust fault in a uniform, perfectly elastic half-space. Slippage on successively shallower segments of this fault plane produces a satisfactory fit to observations. Models with different dips and slip distributions were constructed which fit the data equally well, and more complex models gave better fits, but all showed generally similar features. The amount of slippage given for each of the models used in Fig. 5 is undoubtedly underestimated because of the actual limited east-west extent of the fault. However, except for the 1971 earthquake itself, this extent is not well constrained, so the slip in each model is at best only roughly estimated. Note that slippage from a depth of 25 km to the base of the lithospheric plate is modeled to sufficient accuracy here by slip at all depths below 25 km in the half-space model. Also note that the extent of slippage below 25 km is

not strongly constrained by the available data.

The interpretation presented here is also consistent with the limited amount of leveling carried out adjacent to the line CB (Fig. 4a) from 1965 to 1971 (20). A comparison of elevations in 1968 and 1965 along line AB (Fig. 4a) discloses uplift of 20 mm or less along this profile, deformation that is perhaps attributable to continued sporadic growth of the broad-scale uplift. Alternatively, slip below 25 km on a thrust dipping at an angle shallower than 30° can satisfy both these data and the observations for 1968 and 1965 on CB (Fig. 5a). A comparison of elevations in 1968 and 1969 is available on line BD (Fig. 4a), extending roughly 40 km east from the 1971 epicenter. It shows that the 70-mm uplift of B in this period (Fig. 5b) decreases relatively uniformly to less than 10 mm at D, effectively limiting the eastern extent of this localized uplift (22). Finally, extensive comparisons of 1968 and 1971 observations provide detailed information on the coseismic crustal deformation. These data constrain the absolute level of CB [that is, relative to the Tidal 8 bench mark (T8

in Fig. 4a)] during this interval, a constraint satisfied by the model used in Fig. 5. These data also indicate that the seismic faulting was considerably more complex than that given by the simplified model of Fig. 5: the fault plane dips more steeply than 30°, and irregularities in uplift along the profile CBA require a slip distribution that varies with depth on the fault. Part or even all of the movements from 1969 to 1971 shown in Fig. 5 could be due to preseismic deformation, as has been suggested previously (20).

Episodic Uplift in Other Regions

Two other examples of broad-scale uplift followed by localized vertical deformation and significant thrust-type earthquakes may be similar to the observations from southern California described here. In both cases the available data are sufficient only to suggest similarities: the relevant results come in each instance from a single leveling line following a coastal route nearly parallel to the strike of a causative fault that is located offshore. In addition, some potentially use-

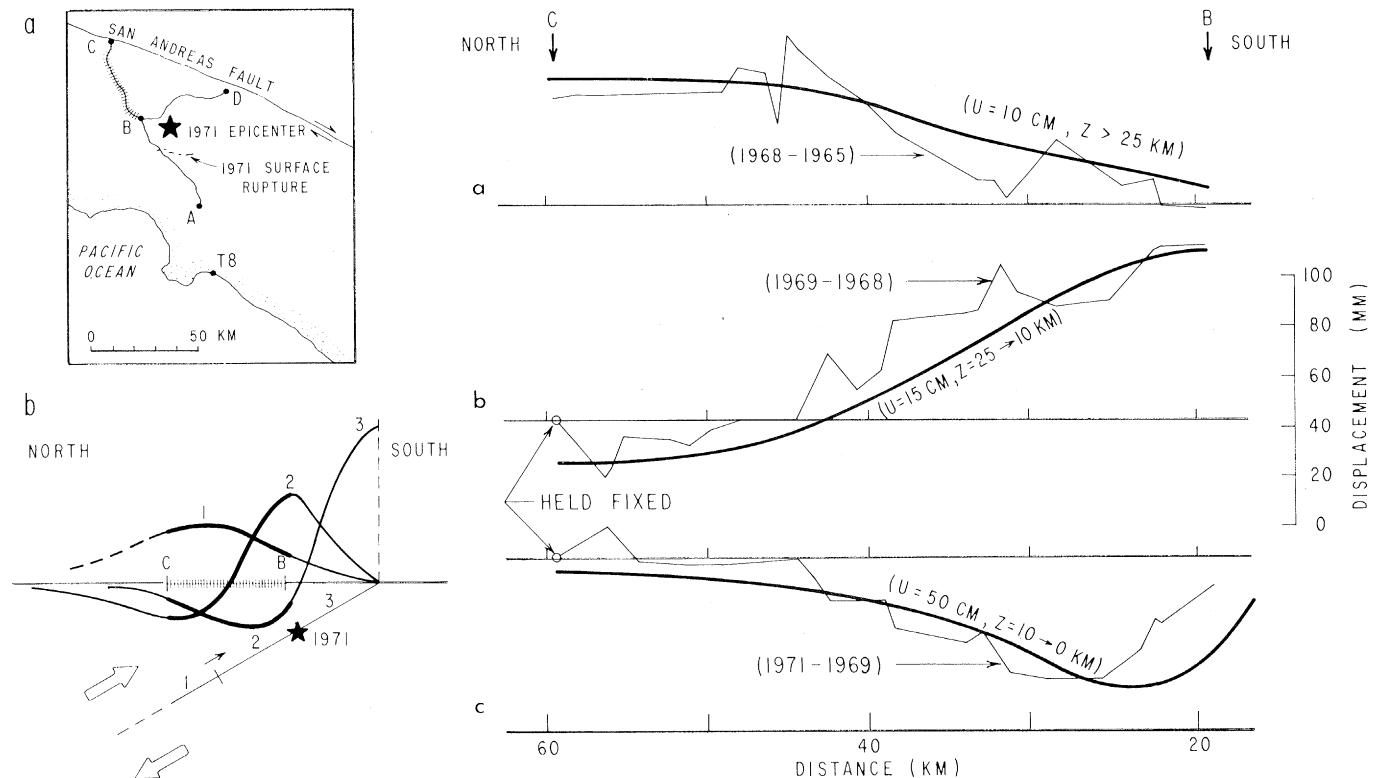


Fig. 4 (left). (a) Location of leveling lines along which localized uplift was observed prior to the 1971 San Fernando earthquake (20). Shown for reference are the 1971 epicenter and surface rupture, and the Tidal 8 bench mark (T8) to which some of this leveling has been tied. Line CB supplies the most significant observations of preseismic uplift, which are plotted in Fig. 5. (b) Schematic plot showing uplift profiles expected from aseismic slip on successively shallower segments of a north-dipping thrust fault lying beneath the section of level line CB and outcropping at the surface trace of the San Fernando fault. The principal effect of this propagating slip is to produce successive sharp reversals in the sense of tilting of the level line CB. Fig. 5 (right). Changes in elevation along the north-south leveling route CB (Fig. 4) for three successive time intervals. Smooth curves show a fit to these data for slippage, U , on successively shallower segments of a 30° north-dipping thrust fault (see Fig. 4b). Depth below the surface is z . (a) The 1968-1965 change (1968 elevation minus 1965 elevation) is tied to the Tidal 8 bench mark (Fig. 4a). No such tie exists for the 1969 leveling, so point C is arbitrarily held fixed in the 1968-1971 profiles (b and c). Horizontal distance is measured north from the surface trace of the San Fernando fault.

ful data are contaminated by the uncertain effects of artificial fluid withdrawal. Such data are excluded from the present discussion.

For the 1964 Niigata, Japan, earthquake of magnitude 7.5, uplift of about 100 mm along most of a 120-km-long leveling route from 1898 to 1955 was succeeded in 1955 to 1958 by sharply episodic upwarping of 50 mm along only 40 km of this line (23). The onshore measurements lie on the lower (footwall) block of the thrust fault more than 20 km from the 1964 surface trace. Although at this location uplift is only a second-order effect of fault slippage, the data for 1955 to 1958 can be fit by several meters of aseismic slip on the fault plane beneath the eventual seismic zone (24).

A second example comes from a 60-km-long portion of a leveling route along coastal southern California that passes within a few kilometers of the epicenter of the 1973 Point Mugu earthquake of magnitude 6.0 (25). Uplift of about 40 mm along this route from 1960 to 1968 was followed by increased localization of deformation toward the eventual 1973 epicenter: downwarping of as much as 40 mm along 45 km from 1968 to 1971, and uplift from 1971 to 1973 that extended along 30 km of the route and reached a maximum of 30 mm near the 1973 epicenter. This latter deformation must have been largely aseismic, since the earthquake itself could have produced no more than a few millimeters of epicentral uplift (25). The 1968–1973 data might be explained by up-dip aseismic slip propagation, but again this interpretation is far from being definitive.

In summary, then, although the data in these two cases are quite limited, the pattern of widespread uplift followed by local preseismic deformation is rather similar to that observed in southern California. Although a convincing case for preearthquake aseismic slip propagation cannot be made with only Niigata and Point Mugu data, such a model is capable of explaining available observations.

Summary

Reexamination of horizontal geodetic data in the region of recently discovered aseismic uplift has demonstrated that equally unusual horizontal crustal deformation accompanied the development of the uplift. During this time interval compressive strains were oriented roughly normal to the San Andreas fault, suggesting that the uplift produced little shear strain accumulation across this fault. On the other hand, the orientation of the

anomalous shear straining is consistent with strain accumulation across north-dipping range-front thrusts like the San Fernando fault. Accordingly, the horizontal and vertical crustal deformation disclosed by geodetic observation is interpreted as a short epoch of rapid strain accumulation on these frontal faults. If this interpretation is correct, thrust-type earthquakes will eventually release the accumulated strains, but the geodetic data examined here cannot be used to estimate when these events might occur.

However, observation of an unusual sequence of tilts prior to 1971 on a level line lying to the north of the magnitude 6.4 San Fernando earthquake offers some promise for precursor monitoring. The data are adequately explained by a simple model of up-dip aseismic slip propagation toward the 1971 epicentral region. These observations and the simple model that accounts for them suggest a conceptually straightforward monitoring scheme to search for similar uplift and tilt precursors within the uplifted region. Such premonitory effects could be detected by a combination of frequently repeated short (30 to 70 km in length) level line measurements, precise gravity traverses, and continuously recording gravimeters sited to the north of the active frontal thrust faults. Once identified, such precursors could be closely followed in space and time, and might then provide effective warnings of impending potentially destructive earthquakes.

References and Notes

1. R. O. Castle, J. P. Church, M. R. Elliott, *Science* **192**, 251 (1976).
2. All of the horizontal control coverage shown in Fig. 1, with the exception of that labeled 1971–75 (3), comprises triangulation measurements made by the U.S. Coast and Geodetic Survey, now the National Geodetic Survey. The observed unadjusted direction lists from these surveys have been made available to me by J. F. Dracup.
3. W. H. Prescott and J. C. Savage, *J. Geophys. Res.* **81**, 4901 (1976).
4. W. S. Dunbar, D. M. Boore, and W. Thatcher [*Eos* **56**, 1067 (1975)] present an analysis of the east-west triangulation arc labeled 1932/52/53/63, data directly relevant to pre-, co-, and post-seismic processes associated with the 1952 Kern County earthquake of magnitude 7.7 (see Fig. 1).
5. F. C. Frank, *Bull. Seismol. Soc. Am.* **56**, 35 (1966). It should be noted that the method used here, in contrast to standard geodetic methods (6, pp. 142–167), does not require that a selected baseline of the network remain invariant in length and orientation between surveys. Relaxation of this restrictive fixed-baseline assumption is important in tectonic regions, since truly stable baselines are rare, and requiring this assumption introduces unknown systematic errors into the results. Note also that the orientation of the horizontal principal compressive and tensile strain axes and their difference in magnitude, which determines the shearing strains, are also determined by the triangulation data and implicitly specified once the magnitude and orientation of the maximum right- or left-lateral shear strains are given. Dilatational strains cannot be determined, since the uniform expansion or contraction of a triangulation network leaves all angles unchanged.
6. G. Bomford, *Geodesy* (Oxford Univ. Press, London, ed. 3, 1971).
7. J. C. Savage and R. O. Burford, *Bull. Seismol. Soc. Am.* **60**, 1877 (1970). To improve the signal-to-noise ratio of the observations, a large number of angle changes, here usually 10 to 30, are used to determine the shear strain rate and orientation by least squares.
8. W. Thatcher, *J. Geophys. Res.* **80**, 4862 (1975).
9. J. C. Savage and W. H. Prescott, *ibid.*, in press.
10. R. Brown, *ibid.*, in press. In these dislocation models of strain accumulation, the fault segment in the bend of the San Andreas may slip at depths below 15 km or be completely locked throughout the thickness of the lithosphere. In either case, the right-lateral shear strain in the bend region close to the fault is approximately parallel to the local trend of the San Andreas within about 30 km of the surface trace. Farther away, as well as near the ends of the locked portion of the fault, the pattern is more complex; here, the uncertain effects of other faults and oversimplicity of the models make comparisons with data more tenuous.
11. Department of Water Resources, *Calif. Dep. Water Resour. Bull.* 116-6 (1968).
12. J. C. Savage, *J. Geophys. Res.* **80**, 4078 (1975).
13. Twelve comparisons with 1959–1967 triangulation measurements made in the same areas show general agreement, although there are several discrepancies larger than the estimated systematic errors of the Geodimeter measurements (12, figure 4, lines 53, 59, and 60). Addition of an arbitrary unknown dilatational strain to the triangulation results can produce agreement between the two data sets, although this is an ad hoc expedient. These remaining discrepancies may well represent larger than anticipated systematic errors in a small number of the early Geodimeter measurements.
14. Note, however, that from the triangulation data used here the magnitude of the compression is determined only relative to the principal tensile strain, and absolute compression may be decreased or even negated by the addition of an arbitrary dilatation.
15. T. Rikitake, *Tectonophysics* **23**, 299 (1974).
16. J. H. Whitcomb, *U.S. Geol. Surv. Prof. Pap.* **733** (1973), p. 30; R. L. Wesson, W. H. K. Lee, J. F. Gibbs, *ibid.*, p. 24.
17. J. C. Jaeger and N. G. W. Cook, *Fundamentals of Rock Mechanics* (Methuen, London, 1969), pp. 369–372. Overcoring measurements carried out at shallow depths have provided consistent values of the orientation of principal stress axes even through the absolute value of the stress is poorly determined. See, for example, R. de la Cruz and C. B. Raleigh, *Int. J. Rock Mech. Min. Sci.* **9**, 625 (1972); E. R. Hoskins, J. E. Russell, K. Beck, D. Mohrman, *Eos* **53**, 1117 (1972). Note, however, that these methods are applicable in the uplifted region only if the stresses relieved by overcoring represent those applied during the most recent deformation episode (and are not, for example, relics of an earlier loading history).
18. H. Kanamori and D. Hadley, *Pure Appl. Geophys.* **113**, 257 (1975).
19. T. C. Hanks, *Geophys. J. R. Astron. Soc.* **23**, 173 (1971). Hanks suggested to me the applicability of this model to the uplifted region.
20. R. O. Castle, J. N. Alt, J. C. Savage, E. I. Balazs, *Geology* **2**, 61 (1974), figure 4 and pp. 64–65.
21. Systematic errors are potentially much greater than accumulated random errors but are very difficult to assess (6, pp. 239–243). Absence of a one-to-one correlation with topography argues against the dominance of systematic errors for the elevation changes shown in Fig. 5.
22. Both Castle *et al.* (20) and J. C. Savage, R. O. Burford, and W. T. Kinoshita [*Calif. Div. Mines Geol. Bull.* **196** (1975), p. 175] have proposed aseismic fault slip at depth to account for the uplift from 1968 to 1969 along the leveling route CBD (Fig. 4a).
23. I. Tsubokawa, T. Dambara, A. Okada, in *General Report on the Niigata Earthquake of 1964*, H. Kawasumi, Ed. (Tokyo Electrical Engineering College Press, Tokyo, 1968), p. 129.
24. This uplift can be produced by fault slippage in at least two ways. First, for a three-dimensional fault, uplift occurs locally as a second-order effect in the region of general downwarping on the footwall block. Second, buried slip on faults dipping at shallower angles beneath the seismic zone will produce similar effects.
25. R. O. Castle, J. P. Church, M. R. Elliott, J. C. Savage, *Bull. Seismol. Soc. Am.*, in press.
26. I am grateful to many colleagues for criticism and stimulating discussion of this work, especially R. O. Castle, J. C. Savage, T. C. Hanks, and C. B. Raleigh.